Human Molecular Genetics, 2008, Vol. 17, No. 1 **119–129**
doi:10.1093/hmg/ddm289
Advance Access published on October 3, 2007

A block of autophagy in lysosomal storage disorders

Carmine Settembre[1,†], Alessandro Fraldi[1,†], Luca Jahreiss[2], Carmine Spampanato[1], Consuelo Venturi[3,4], Diego Medina[1], Raquel de Pablo[1], Carlo Tacchetti[3,4], David C. Rubinsztein[2,‡] and Andrea Ballabio[1,5,*]

[1]Telethon Institute of Genetics and Medicine (TIGEM), Naples, Italy [2]Department of Medical Genetics, Cambridge Institute for Medical Research, Cambridge, UK [3]Department of Experimental Medicine and [4]MicroSCoBiO Research Center and IFOM Center of Cell Oncology and Ultrastructure, University of Genoa, Genoa, Italy and [5]Medical Genetics, Department of Pediatrics, Federico II University, Naples, Italy

Received August 5, 2007; Revised and Accepted September 30, 2007

Most lysosomal storage disorders (LSDs) are caused by deficiencies of lysosomal hydrolases. While LSDs were among the first inherited diseases for which the underlying biochemical defects were identified, the mechanisms from enzyme deficiency to cell death are poorly understood. Here we show that lysosomal storage impairs autophagic delivery of bulk cytosolic contents to lysosomes. By studying the mouse models of two LSDs associated with severe neurodegeneration, multiple sulfatase deficiency (MSD) and mucopolysaccharidosis type IIIA (MPSIIIA), we observed an accumulation of autophagosomes resulting from defective autophagosome-lysosome fusion. An impairment of the autophagic pathway was demonstrated by the inefficient degradation of exogenous aggregate-prone proteins (i.e. expanded huntingtin and mutated alpha-synuclein) in cells from LSD mice. This impairment resulted in massive accumulation of polyubiquitinated proteins and of dysfunctional mitochondria which are the putative mediators of cell death. These data identify LSDs as 'autophagy disorders' and suggest the presence of common mechanisms in the pathogenesis of these and other neurodegenerative diseases.

INTRODUCTION

Deficiencies of specific lysosomal hydrolases in lysosomal storage disorders (LSDs) cause accumulation of their undegraded target substrates. However, it is not clear if these substrates themselves are the primary mediators of toxicity. Indeed, the biological pathways from lysosomal enzyme deficiency to cellular dysfunction are still largely unknown (1,2). Interestingly, despite the great structural diversity of the accumulating substrates in the different LSDs, these disorders share many phenotypic similarities, suggesting the presence of common pathogenetic mechanisms. Many LSDs are associated with progressive and severe neurodegeneration which represents the most difficult challenge for their therapy (2). In previous studies, we detected severe neurodegeneration in murine models of mucopolysaccharidoses type II and IIIA (MPSII and MPSIIIA, respectively) and of multiple sulfatase deficiency (MSD) (3–6).

The degradation of intracellular proteins is performed by two major mechanisms: the ubiquitin-proteasome system (UPS) and macroautophagy (hereafter referred to as autophagy). The latter is a lysosomal-dependent catabolic pathway through which long-lived cytosolic proteins and organelles, such as mitochondria, are sequestered by double membrane vesicles (autophagosomes) and ultimately degraded after autophagosome-lysosome fusion (7). Many of the aggregate-prone proteins causing late-onset neurodegenerative conditions, such as Huntington's and familial forms of Parkinson's

*To whom correspondence should be addressed at: Telethon Institute of Genetics and Medicine (TIGEM), Via P. Castellino 111, 80131 Napoli, Italy. Tel: +39 0816132207; Fax: +39 0815790919; Email: ballabio@tigem.it
†The authors wish it to be known that, in their opinion, the first two authors should be regarded as joint First Authors.
‡Both D.C.R. and A.B. should be regarded as senior authors.

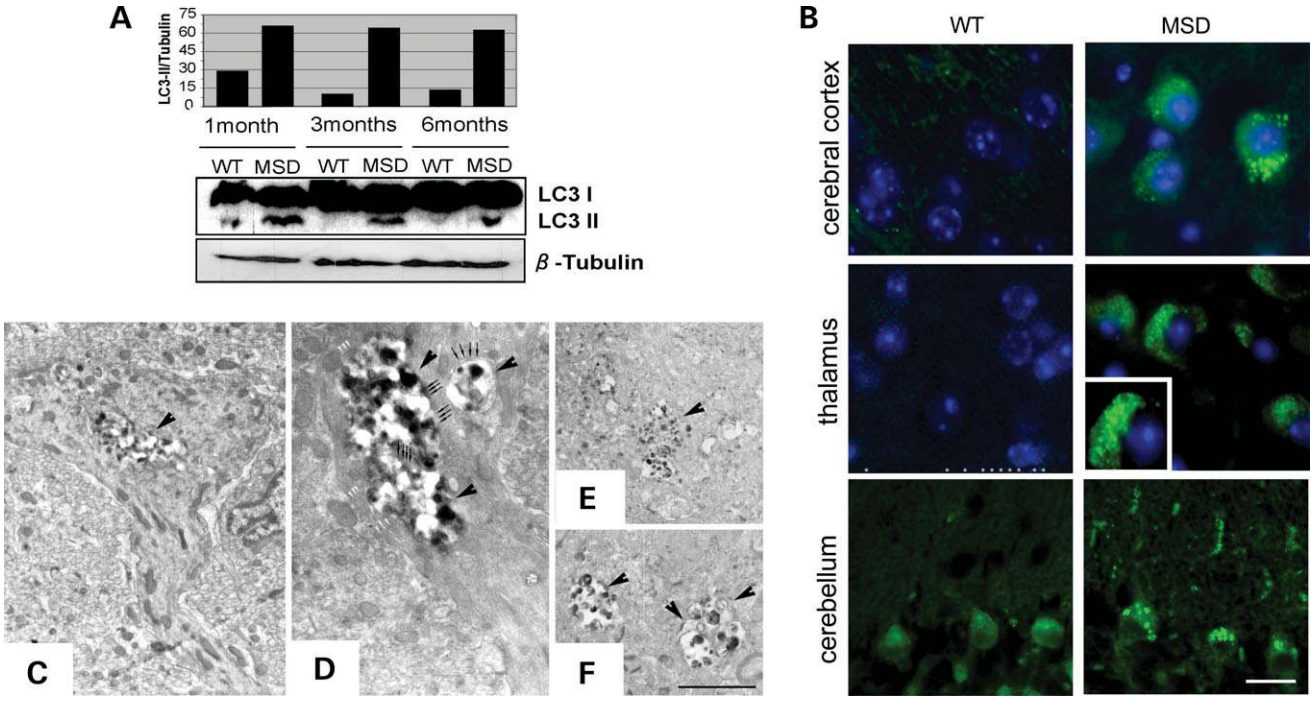

Figure 1. Accumulation of autophagosomes in MSD brain. (**A**) Anti-LC3 western blot of total brain homogenates prepared from 1, 3 and 6-month-old MSD and wild-type mice. (**B**) Immuno-fluorescence staining of LC3 in different brain regions of MSD mice and wild-type littermates. Bar = 15 μm. (**C**–**F**) Electron micrographs of both cerebellum (C and D) and cerebral cortex (E and F) from an MSD mouse. A neural process from a Purkinje cell, containing a large autophagosome (black arrowhead) and an enlargement of a portion of a neural process from a Purkinje cell are shown in (C). (D) Three autophagosomes (black arrowheads) in Purkinje cells surrounded by a double membrane (arrows) and containing remnants of cellular organelles. Membrane cisterns pile up in stacks (white arrowheads) by the autophagosomes. (E and F) Electron micrographs of autophagosomes (black arrowheads) in cerebral cortex. Bar: $d = 3.0$ μm; $e = 1.6$ μm; $f = 9.3$ μm; $g = 5.6$ μm.

diseases, are autophagy substrates (8). In addition, knock-out of autophagy genes causes abnormal protein accumulation in ubiquitinated inclusions and neurodegeneration in mice (9,10).

We hypothesized that LSDs are associated with a lysosomal dysfunction that impairs the autophagic pathway ultimately leading to cell death. To test this hypothesis, we studied the mouse models of two LSDs: MSD, which is caused by the deficiency of the sulfatase modifying factor 1 (*SUMF1*) gene involved in the post-translational modification of sulfatases (6,11,12), and MPS-IIIA, caused by sulfamidase deficiency (13). Our results revealed a block of autophagic pathway occurs as a consequence of decreased ability of lysosomes to fuse with autophagosomes. This results in the cellular accumulation of toxic substrates which are the putative mediators of cell death.

RESULTS

Increased autophagosome number in MSD

We assessed autophagosome number in brain sections from MSD mice by using an antibody detecting the autophagosome marker LC3 (14). During autophagosome formation, the LC3-I isoform is converted into LC3-II, whose amount (compared to actin or tubulin) correlates with the number of autophagosomes (14). LC3-II is the only known protein that specifically associates with autophagosomes and not with other vesicular structures. LC3-II levels were clearly raised in whole brain homogenates from MSD mice, compared to wild-type littermates at 1, 3 and 6 months of age (Fig. 1A). Furthermore, immuno-fluorescence analysis revealed increased numbers of LC3-positive vesicles in the cerebral cortex, cerebellum and thalamus of MSD mice, compared to corresponding brain regions of wild-type mice (Fig. 1B). Electron microscopy evaluation of cerebellum (Fig. 1C and D) and cerebral cortex (Fig. 1E and F) sections from MSD mice showed abnormally abundant autophagosomes. Interestingly, the morphology of autophagic vacuoles accumulating in MSD mice resembled that of early immature autophagosomes (15,16) (Fig. 1C–F), suggesting the presence of a defective maturation.

A similar increase in LC3-II levels was observed in mouse embryonic fibroblasts (MEFs) and embryonic liver macrophages (ELMs) (Fig. 2A)—macrophages were previously identified as the primary site of lysosomal storage in MSD mice (6). The increase in both number and size of autophagosomes was confirmed in MEFs by quantitative analysis (Fig. 2B and C).

Autophagosome-lysosome fusion is impaired in MSD

Clearance of autophagosomes occurs via fusion with lysosomes. We postulated that accumulation of autophagosomes

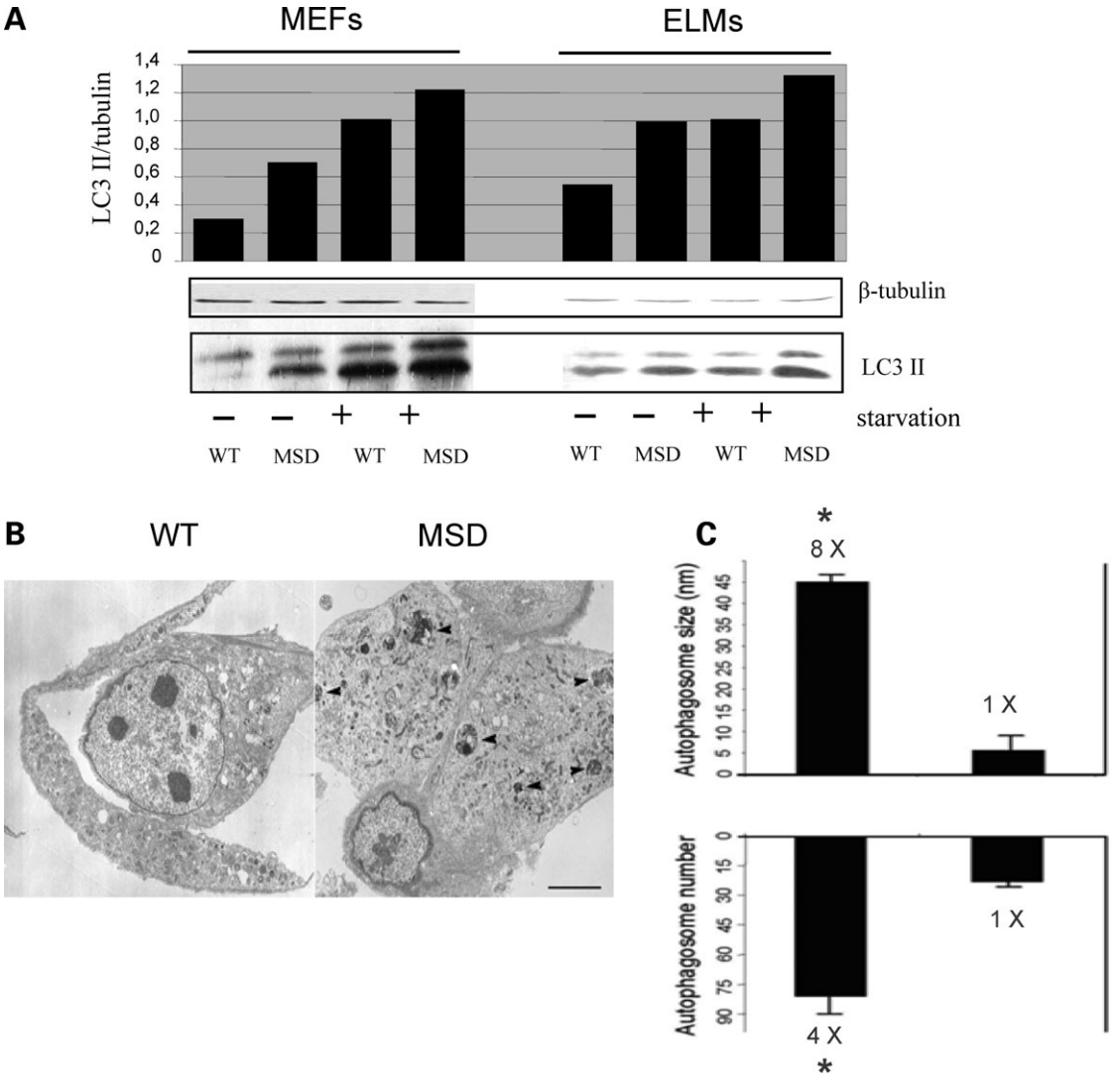

Figure 2. Accumulation of autophagosomes in MSD cultured cells. (**A**) Anti-LC3 western blot of protein extracts prepared from MEFs and ELMs derived from MSD and wild-type mice in both normal and starved conditions. (**B**) MSD MEFs display several autophagosomes (arrowheads), compared to wild-type. Bar = 9.3 μm. (**C**) Morphometric evaluation revealed that autophasomes were more numerous and larger in MSD MEFs compared to those observed in wild-type MEFs. $^{*}P < 0.05$.

in MSD is due to defective clearance caused by impaired autophagosome-lysosome fusion. To test this hypothesis, we analyzed the subcellular localization of the lysosomal marker lgp120 (LAMP1) and the autophagosomal marker LC3 by confocal microscopy. These experiments demonstrated that the extent of lgp120/LC3 co-localization was significantly reduced (ranging from 40 to 50%) in MSD compared to wild-type MEFs, thus indicating impaired autophagosome-lysosome fusion (Fig. 3A and B). This was observed both in normal medium (basal autophagy) (Fig. 3A) and in starved cells (induced autophagy) (Fig. 3B).

To characterize this impairment, we used drugs which either induce or inhibit autophagy. Autophagy stimulation with rapamycin increased LC3-II levels in both MSD and wild-type MEFs (Fig. 4). Moreover, LC3-II levels in MSD MEFs were further increased with bafilomycin A1, an inhibitor autophagosome-lysosome fusion (17), alone or in combination with rapamycin, suggesting that the block of autophagy is not complete (Fig. 4).

Decreased ability of MSD cells to degrade exogenous aggregate-prone proteins

Defective autophagosome-lysosome fusion may lead to an impairment of autophagy. We investigated the ability of MSD cells to degrade aggregate-prone proteins which are autophagy substrates (18). These include the mutant huntingtin and A53T α-synuclein which are involved in Huntington and familial Parkinson diseases, respectively. Mutant huntingtin exon 1 constructs aggregate readily in tissue culture and form inclusions readily visible by light microscopy. The proportion of cells with such inclusion is linearly related to the expression levels of the construct (19). The A53T α-synuclein construct does not form overt inclusions in the cell lines we

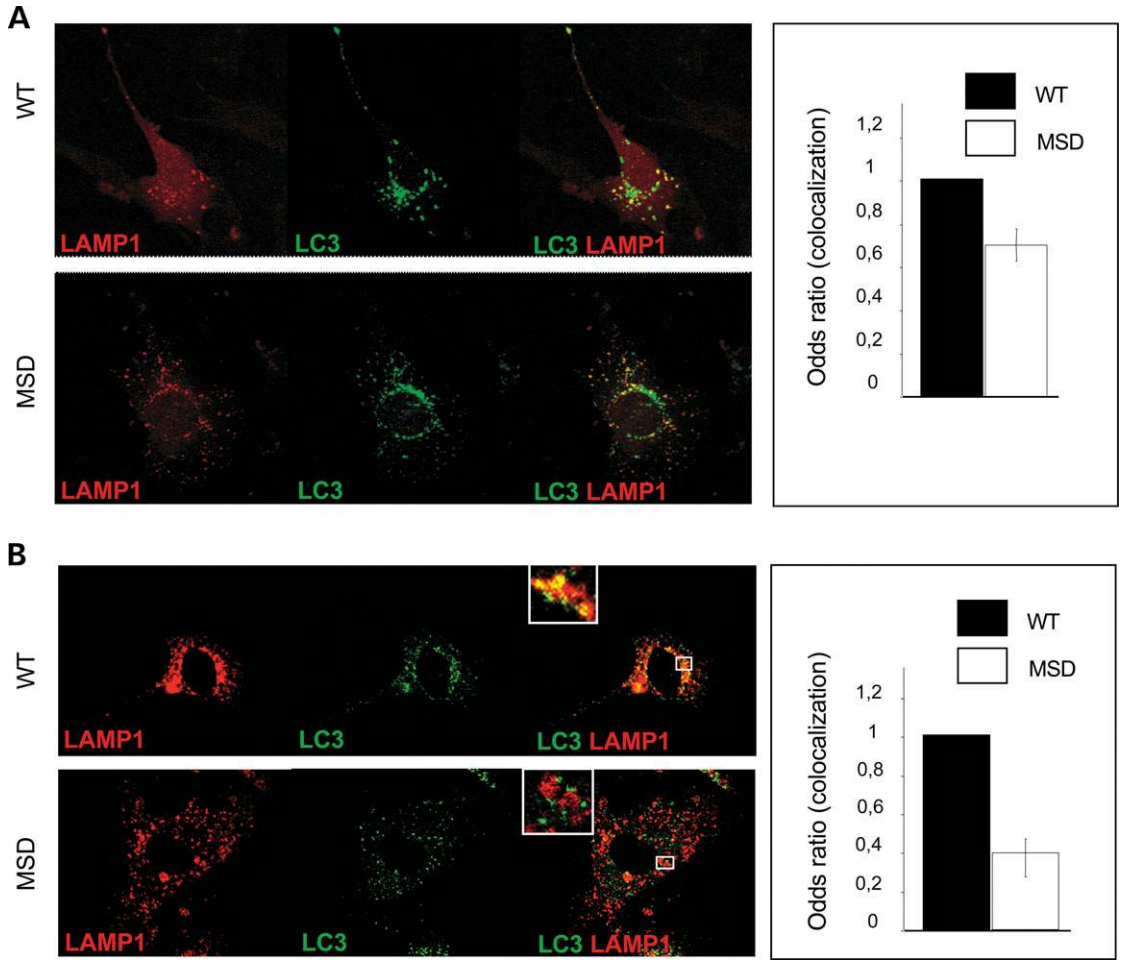

Figure 3. Defective autophagosome-lysosome fusion in MSD MEFs. (**A** and **B**) Co-localization of LAMP1 and LC3 in wild-type and MSD MEFs stained for LAMP1 (red) and LC3 (green). Confocal microscopy shows a reduction in the extent of co-localization of LAMP1 and LC3 proteins. The figure was selected to illustrate the basis for the assays we have quantified. The number of autophagosome-lysosome fusion events in MSD MEFs was quantified both in normal (A) and starved (B) serum conditions, as described in the Methods section.

have studied (20). We expressed these mutant proteins in MSD cells to test the functionality of the autophagic pathway. The Gln_{74};Q74 huntingtin, which encodes the first exon of huntingtin with 74 glutamine repeats, and the A53T α-synuclein were fused to green fluorescent protein (GFP) and transiently expressed in both MEFs and ELMs derived from MSD mice. Forty-eight hours after transfection, cells were collected and GFP-fused proteins were detected by western blot. Figure 5A shows an increased accumulation of both types of mutant proteins in MSD compared to wild-type cells. In addition, immuno-fluorescence analysis revealed that the number of GFP-Q74 aggregates was also significantly higher in MSD MEFs and ELMs compared to wild-type cells (Fig. 5B and C). Notably, when cells were analyzed at earlier time points, no significant differences in the accumulation of GFP-Q74 were observed between wild-type and MSD cells (Supplementary Material), this indicating that only at later time points accumulation of overexpressed proteins occurs. Moreover, GFP alone did not accumulate in MSD cells (Supplementary Material) demonstrating that increased levels of GFP-Q74 and GFP-A53T are due to autophagic defective degradation and not to difference in transfection efficiency.

Taken together, these data indicate a dysfunction of autophagy with consequent decreased ability of MSD cells to degrade aggregate-prone proteins.

Polyubiquitinated proteins progressively accumulate in MSD neurons

Autophagy is responsible for constitutive protein turnover (8). This function appears to be particularly important in neuronal cells and is relevant to neurodegenerative diseases (21,22). Knockout of autophagy genes results in suppression of autophagy and accumulation of inclusion bodies, which contain polyubiquitinated proteins, in neurons (9,10). We detected a massive and progressive accumulation of ubiquitin-positive inclusions in the cerebral cortex as well as in other brain regions of MSD mice by both anti Ub immuno-histochemical and immuno-fluorescence analyses (Fig. 6A and B and data not shown). Co-localization of Ubiquitin with NeuN neuronal marker indicates that

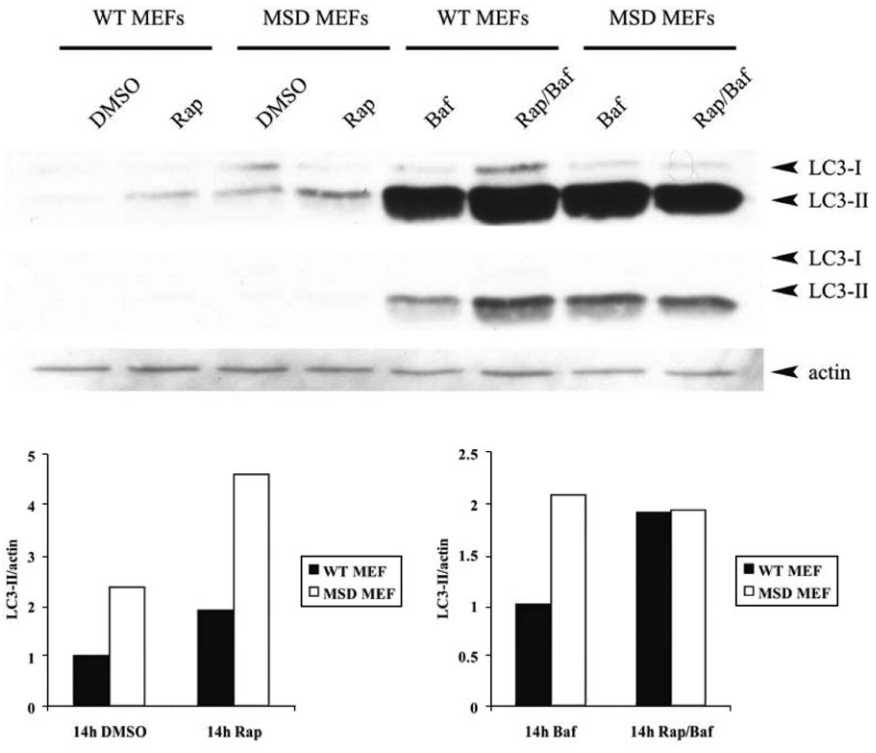

Figure 4. Evaluation of LC3 levels in MSD and wild-type MEFs after induction and/or inhibition of autophagy. Both wild-type and MSD MEFs were treated with indicated drugs. Western-blot analysis (top) was performed using anti-LC3 antibodies. Quantitation (bottom) was performed by normalizing with actin levels. The middle lane in the western blot is a lower exposure of the upper lane.

ubiquitin inclusions are located in neurons (Fig. 6B). Progressive accumulation of polyubiquitinated proteins was also detected by western blotting of brain homogenates (Fig. 6C). Importantly, analysis of chymotrypsin-like proteasome activity in MSD brain at several ages revealed that proteasome function is not affected in MSD mice (data not shown), indicating that the accumulation of ubiquitinated proteins is due to defective autophagy rather than to UPS impairment.

In addition, we found that P62/SQSTM1 significantly accumulates (Fig. 6D), and co-localizes with ubiquitin-positive inclusions (Fig. 6E) in brain from MSD mice. The p62/SQSTM1 protein is known to be a common component of ubiquitin-positive protein aggregates in neurodegenerative diseases (23), being involved in the targeting of polyubiquitinated proteins to the autophagosomes and selectively degraded via the autophagic pathway (24).

Accumulation of dysfunctional mitochondria in MSD mice

Autophagy also plays a crucial role in the degradation and turnover of cellular organelles like mitochondria. Indeed, it has been suggested that autophagy selectively degrades dysfunctional mitochondria (25). Fragmented and dysfunctional mitochondria have been reported to accumulate in patients with mucolipidosis types II, III and IV and in patients with neuronal ceroid lipofuscinosis 2 (NCL2), suggesting that lysosomal storage in these diseases impairs autophagy-mediated mitochondrial turnover (26,27). Electron microscopy analysis revealed an increased number of mitochondria in MSD brain sections and MEFs (Fig. 7A and B). Consistently, an increase of Cox4 (a mitochondrial marker) levels was detected by western blotting in MSD brain samples (Fig. 7C). To examine the function of accumulating mitochondria, we measured the mitochondrial membrane potential ($\Delta\Psi m$) in WT and MSD MEFs by using a mitochondria-specific voltage dependent dye ($DiOC_6$). As shown in Fig. 7D, MSD MEFs show a significant reduction in the $\Delta\Psi m$ compared to wild-type cells in both normal and starved conditions, thus indicating that mitochondria accumulating in MSD are dysfunctional.

Impairment of autophagy in MPSIIIA

Overall, our data identify an impairment of autophagy in MSD, leading to the accumulation of polyubiquitinated proteins and of dysfunctional mitochondria. To investigate whether this applies to other LSDs caused by defective hydrolases, we analyzed the autophagic pathway in the murine model of MPSIIIA, which is also associated with severe neurodegeneration (4,5). The results obtained in MPSIIIA mice were similar to those of MSD mice. We detected increased LC3II levels in MPSIIIA MEFs (Fig. 8A) as well as accumulation of autophagosomes in brain samples (Fig. 8B). Consequently, accumulation of ubiquitin-positive inclusions (Fig. 8C) and P62/SQSTM1 (Fig. 8D) were observed in the brain of MPSIIIA mice. In addition, electron microscopy analysis revealed an increased number of mitochondria in

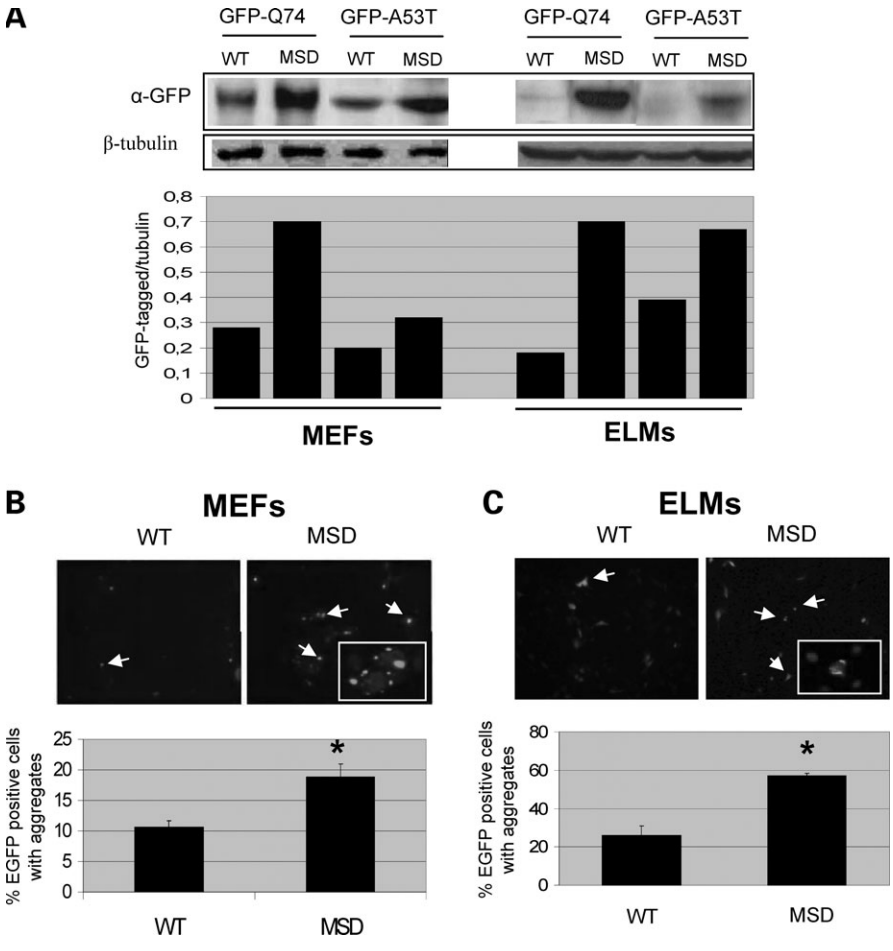

Figure 5. Decreased ability of MSD cells to degrade exogenous aggregate-prone proteins. (**A**) Gln_{74};Q74 huntingtin (encoding the first exon of expanded huntingtin containing 74 glutamine repeats) or A53T α-synuclein were transiently expressed (48 h) as GFP-tagged proteins along with GFP (GFP proteins:GFP 1,5:1 ratio) in both MEFs and ELMs derived from MSD and wild-type mice. The amount of GFP-Q74 and GFP-A53T proteins was then assessed by anti-GFP western blot. (**B** and **C**) Fluorescence microscopy evaluation of GFP-aggregates in MEFs (B) and ELMs (C) expressing GFP-Q74 huntingtin. Transfected MSD MEFs and ELMs displayed a significant increase in percentage of GFP-positive cell containing aggregates compared to transfected wild-type cells. Cell counts were performed on three independent experiments and 50 cells were analyzed in each experiment. $^{*}P < 0.05$.

MPSIIIA brain (data not shown). Similarly to MSD, accumulation of toxic substrates was observed in the absence of any detectable impairment of proteasome function (data not shown).

DISCUSSION

Mucopolysaccharidoses represent a substantial proportion (∼25%) of all LSDs (28). Our results in MSD and MPSIIIA indicate that lysosomal storage in these diseases causes cellular dysfunction by blocking autophagic protein clearance. We provide evidence for this block at both structural (i.e. defective autophagosome-lysosome fusion) and functional levels (i.e. impaired ability of cells to degrade exogenous aggregate-prone proteins, and accumulation of endogenous substrates, such as ubiquitinated proteins, P62 and mitochondria).

Accumulation of ubiquitinated proteins was also observed in mice with autophagy gene knockouts and likely results from increased ubiquitination of substrates by virtue of their longer half-lives. These mice show severe neurodegeneration, suggesting that neurons, compared to other cell types, are more susceptible to a block of autophagy. This may be because non-mitotic cells cannot dilute accumulating cytosolic contents by cell division. This may also explain the prevalence of a neurological phenotype in LSDs.

Furthermore, our data provide an explanation for previous reports of autophagosome accumulation in other types of LSDs, namely Danon disease (15), NCL2 (26,29), Glycogenosis type II (Pompe disease) (30) and Mucolipidosis IV (27). Note that these previous studies did not resolve the crucial issue if the autophagosome accumulation was due to increased formation of autophagosomes (which would lead to increased degradation of autophagic substrates), or decreased autophagosome-lysosome fusion (which results in decreased degradation of such substrates). Clearly, these different scenarios result in vastly different pathological consequences. An induction, rather than a block, of autophagy was observed in NPC types 1 and 2, associated with increased levels of beclin-1 expression (31,32). However, NPC represents the 'atypical' type of LSD as it is caused by mutations in cholesterol transporters, thus suggesting a direct role of lipid

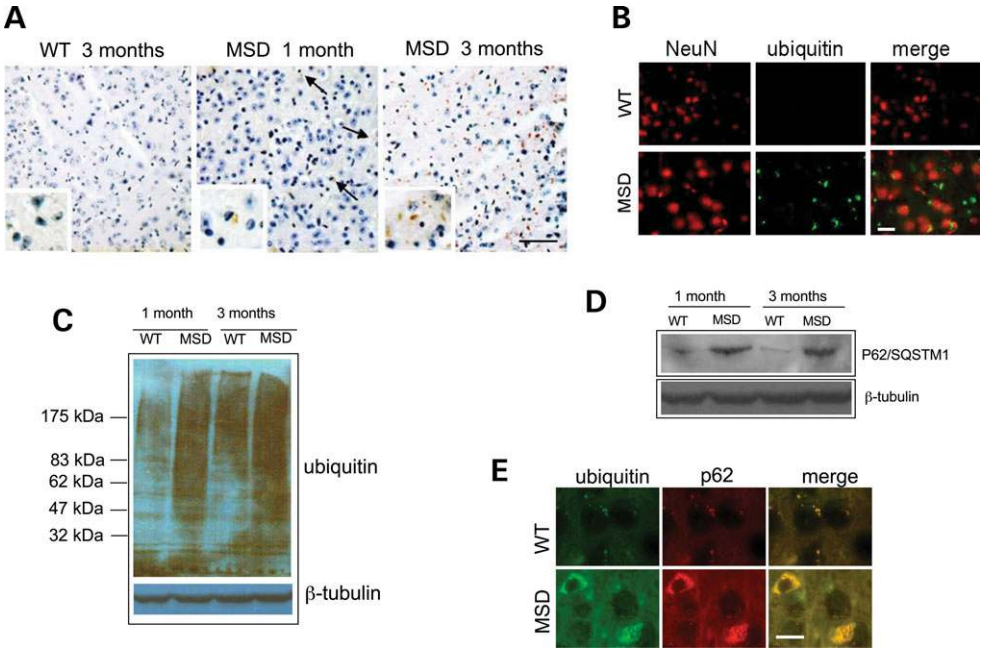

Figure 6. Accumulation of ubiquitin-positive inclusions and of P62 in MSD brain. (**A**) Immuno-histochemical staining of ubiquitinated proteins in the cerebral cortex of a 1-month-old wild-type mouse and of 1 and 3 month-old MSD mice. Bar = 30 μm. (**B**) Anti-Ub (green) and anti-NeuN (red) immuno-fluorecence of cerebral cortex sections derived from MSD and wild-type mice showing the presence of ubiquitin-positive inclusions in MSD neurons. Bar = 20 μm. (**C**) Anti-Ub western blot from total brain homogenates derived from 1 and 3 month-old MSD mice and wild-type littermates. (**D**) Western blot analysis of total brain homogenates showing progressive accumulation of P62 in MSD. (**E**) Immuno-fluorescence with anti-P62 (red) and anti-Ub (green) showed significant co-localization of P62 with polyubiquitinated proteins in the brain of MSD mice. Bar = 12 μm.

trafficking in the regulation of autophagy (32). Accordingly, we found no differences in beclin-1 expression between tissues from MSD mice and wild-type littermates (data not shown).

We propose a model which identifies a block of autophagy as a crucial component in the pathogenesis of LSDs (Fig. 9). According to this model, lysosomal accumulation of undegraded substrates results in defective fusion between autophagosomes and lysosomes and causes a block of the autophagic pathway. As a consequence of this block, toxic proteins and dysfuctional mitochondria accumulate, ultimately leading to apoptosis, either directly or through the induction of chronic inflammation and cytokine release (6). Indeed, cells with impaired autophagy have an increased susceptibility to mitochondria-mediated apoptosis (33,34). It is interesting to note that bafilomycin A1, a proton-pump inhibitor which attenuates lysosomal acidification, results in similar blocks in autophagosome-lysosome fusion as LSDs, suggesting that there may be ways that defective lysosomal function feed back to inhibit autophagosome-lysosome fusion.

Importantly, we found that the ubiquitin-proteasome degradation is not impaired in our LSD mouse models. Proteasome dysfunction may lead to the accumulation of ubiquitinated inclusions (35) and has been associated to neurodegenerative diseases (36–38). The finding that UPS is functional in our LSD models allows us to conclude that the block of autophagy pathway is the only mechanism accounting for the accumulation of ubiquitinated proteins which are the putative mediators of cell death in LSDs. Interestingly, a recent work from Pandey *et al*. (39) showed that autophagy and proteasome are compensatory interacting systems, and pointed to the role of autophagy in rescuing protein degradation deficiency due to the proteasome impairment. This finding raises the possibility to exploit new therapeutic approaches for LSDs based on pharmacological induction of proteasome function in order to compensate for autophagy deficiency.

Our model defines LSDs as 'autophagy disorders', resembling more common neurodegenerative diseases such as Alzheimer (AD), Parkinson (PD) and Huntington (HD) diseases. While there are major differences in the initial steps involved in all these diseases (i.e. impaired degradation of polyubiquitinated proteins in LSDs versus expression of aggregate-prone proteins in AD, PD and HD), our data suggest that they may share common mechanisms suggesting the possibility of overlapping therapeutic strategies.

METHODS

Generation of MEFs and ELMs

MEFs were isolated by trypsinization of littermate embryos isolated at E14 and grown in DMEM supplemented with 20% FBS and penicillin/streptomycin. Fetal liver cells were isolated from E14.5 embryos by mechanical homogenization and filtering through a 40 μm cell-strained. The cells were resuspended in DMEM plus 10% fetal bovine serum and allowed to attach to plastic. Adherent macrophages (obtained by washing wells in DMEM to remove non-adherent cells) were cultured in macrophage medium (PAA) and repurified by immune-separation using CD11b-coating magnetic beads

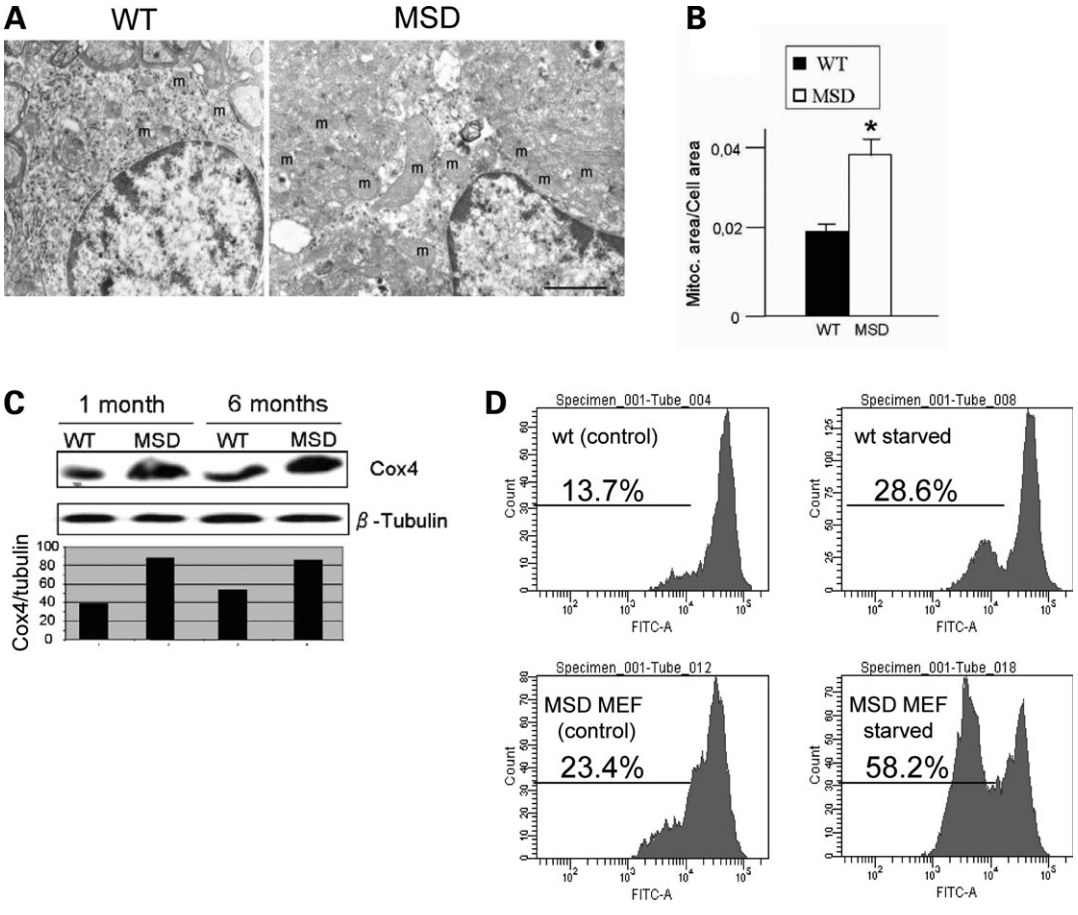

Figure 7. Accumulation of dysfunctional mitochondria in MEFs and brain of MSD mice. (**A** and **B**) Electron microscopy analysis of the brain cortex neurons from MSD mice and wild-type littermates (bar: wild-type = 2.1 μm; MSD = 1.8 μm). MSD neurons contain a significantly higher number of mitochondria (m) compared to wild type neurons as also evident from quantitative analysis (B) (*$P < 0.05$). (**C**) Western blot analysis using antibodies recognizing Cox4, a mitochondrial marker, shows increased levels of Cox4 in MSD compared to wild-type MEFs. (**D**) Wild-type and MSD MEFs were grown in either normal serum or starved conditions (4 h). Cells were then stained with 40 nM DiOC6 and 1 μg/ml propidium iodine. Δ*Y*m was measured by flow cytometry. Propidium iodine was used as counterstain. All experiments were performed in triplicate and analyzed using Stat-View software and ANOVA test. Results were considered significant if $P < 0.05$.

(MACs technology, Miltenyi Biotec). Macrophages were characterized by the expression of MOMA-2, and F4/80 antigens by immuno-fluorescence.

Transfections and drug treatments

Sub-confluent cells (MEFs or ELMs) were transfected using lipofectamine™ 2000 (Invitrogen) according manufacturer's protocols. For co-localization experiments in normal serum conditions, sub-confluent MEFs were co-transfected with 0.5 μg lgp120-GFP and 1 μg mCherry-LC3mCherry-LC3 and cultured in full medium for 24 h. For drug treatments, cells were treated for 14 h with 0.2 mg/ml rapamycin (Sigma), 200 nM bafilomycin A1 (Upstate).

Cloning of mCherry-hLC3B construct

Human LC3B was subcloned from pGEX-6P-1 into pcDNA3 (Invitrogen) using BamHI and EcoRI (both NEB). mCherry pRSET-B was amplified by PCR with the following primers: 5'-TA CCG AGC TCG GTA CCC GCC ACC AT-3' and 3'-G CTG TAC AAG CAA GGA TCC TGC-5'. The resulting fragments were purified, digested with KpnI and EcoRI (both NEB) and sub-cloned in frame into the 5' end of hLC3B pcDNA3.

Antibodies

Primary antibodies were: rabbit polyclonal anti-LC3 (Novus Biological), rat monoclonal anti-mouse LAMP1 (Developmental Studies Hybridoma Bank, Iowa), rabbit polyclonal anti-ubiquitin (DakoCytomation), mouse monoclonal anti-NeuN (Chemicon), mouse monoclonal P62/SQSTM1 (BD), rabbit polyclonal anti-tubulin (Cell signaling), rabbit polyclonal anti-actin (Sigma) and mouse monoclonal anti-COX4 (Clontech). Secondary antibodies were: goat anti-rabbit or anti-rat conjugated to Alexa Fluor 488 or 594 (Molecular Probes, Eugene, OR, USA). HRP-conjugated anti-mouse or anti-rabbit IgG (Amersham); biotinylated donkey anti-rabbit (Jackson ImmunoReasearch).

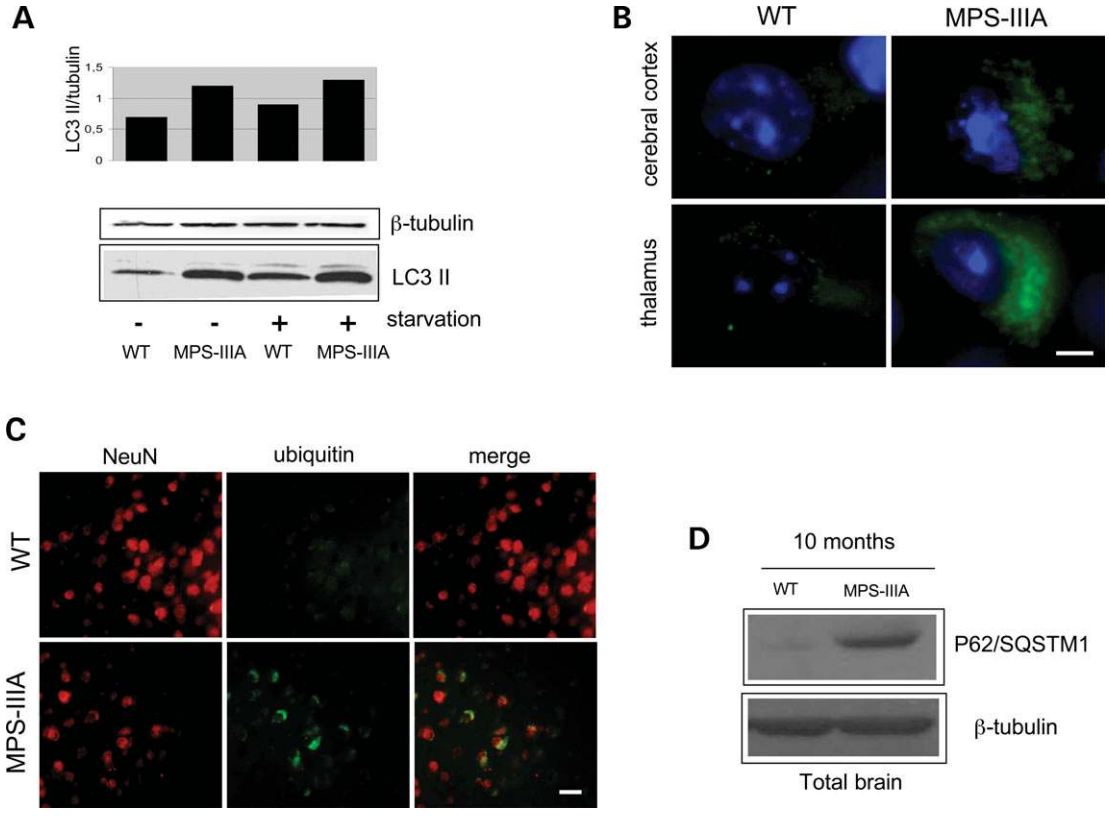

Figure 8. Autophagy impairment in MPSIIIA mice. (**A**) Anti-LC3 western blot of MPSIIIA and wild-type MEFs in either normal or starved serum conditions. Quantification of LC3 protein levels shows an increase of the LC3-II isoform in MPSIIIA MEFs in either normal or starved serum conditions. (**B**) Immuno-fluorescence staining of LC3 in the thalamus and cerebral cortex of MPSIIIA and wild-type mice. Bar = 7 μm. (**C**) Anti-Ub immuno-fluorescence analysis of MPSIIIA mouse brain showing accumulation of ubiquitinated proteins (green) in neurons (NeuN marker:red). Bar = 20 μm. (**D**) Anti-P62 western blot of total brain homogenates from MPSIIIA and wild-type mice. The levels of P62 protein are significantly higher in MPSIIIA mouse brain.

Western blot

Cells were lysed in cold lysis buffer (20 mM Tris–HCl, pH 7.4,150 mM NaCl, 1% TritonX-100) in the presence of protease inhibitors (Roche Diagnostics) for 30 min on ice. Brain tissue samples were homogenized in sucrose buffer, centrifuged and resulting supernatants lysed in TritonX-100. Proteins were transferred onto nitrocellulose membrane (Amersham Pharmacia Biotech). Primary and (HRP)-conjugated antibodies were diluted in 5% milk. Bands were visualized using the ECL detection reagent (Pierce). Proteins were quantified by the Bradford method.

GFP analysis and immuno-staining

Cells were grown on coverslips and fixed in PBS pH 7.4 4% paraformaldehyde (GFP analysis) for 20 min. Tissues were fixed overnight in PBS pH 7.4 4% paraformaldehyde and were embedded in optimal cutting temperature compound (Tissue Tek). Cryostat sections were cut at 10 mM. For immuno-fluorescence analysis, cells/tissues were permeabilized and incubated with appropriate primary and secondary antibodies (diluted in PBS+1% FBS). Immuno-histochemistry was performed using Vectastain ABC kit (Vector Laboratories, Burlingame, CA, USA) according to standard protocols. Cells/tissue slides were mounted and cover-slipped in glycerol/DAPI and viewed on an epi-fluorescent microscope or counterstained with hematoxylin and viewed on a light microscope (immuno-histochemical analysis).

Confocal microscopy

For co-localization analysis in normal serum conditions, cover slips were blinded and 20 cells per cell line per experiment were imaged on a Zeiss Axiovert 200 M microscope with a LSM 510 confocal attachment using a ×63 1.4 NA Plan Apochromat oil-immersion lens. Laser lines at 488 nm (lgp120-GFP) and 543 nm (mCherry-LC3) were used. The detector pinholes were set to give a 0.9 μm optical slice. Acquisition was performed using Zeiss LSM 510 software. These cells were then analysed in *Zeiss LSM Image Browser 3.5* as follows: first, only mCherry-LC3+ vesicles were counted and marked, by switching off the GFP-channel. Then, the GFP-channel was switched back on and the number of co-localized vesicles was counted. From these two values, the fraction of co-localized vesicles was then determined. The number of autophagosome-lysosome fusion events in starved MSD and wild-type MEFs were determined by the analysis of confocal images [obtained by a Leica TCS SP2 AOBS confocal microscope with a ×63 Neofluor Pan-Apo 1.3 nm oil objective with laser lines at 488 nm (LC3) and 594 nm (LAMP1)] utilizing Volocity 3.7.0 software

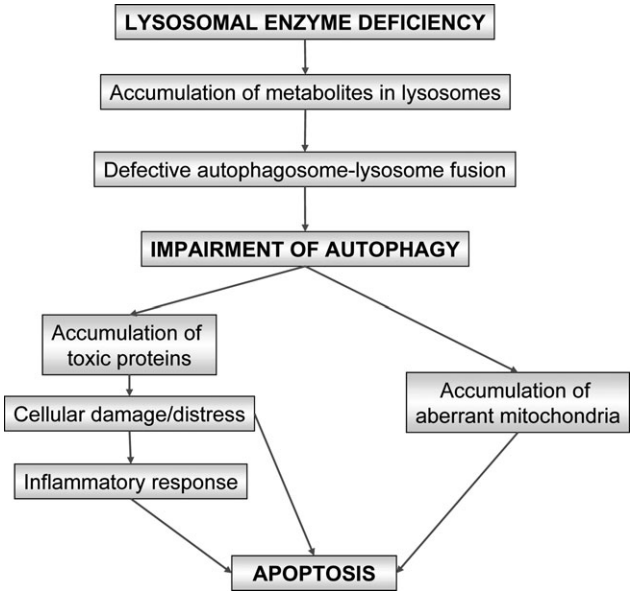

Figure 9. A proposed model for the pathogenesis of LSDs. A defect in lysosomal degradation results in the accumulation of substrates in the lysosomes. Lysosomal storage leads to a reduced ability of lysosomes to fuse with autophagosomes with a consequent block of autophagy. Polyubiquitinated protein aggregates and dysfunctional mitochondria accumulate and promote apoptosis-mediated cell death. The inflammatory response to cell damage further contributes to cell death.

(Improvision). Pearson's correlation was used as a value of co-localization between autophagosomes and lysosomes.

Mitochondrial membrane potential measurements

PBS-washed 1×10^6 cells were incubated in 40 nM $DiOC_6$ (Sigma-Aldrich) and 1 μg/ml PI (Sigma-Aldrich) for 15 min at 37°C. After washing, cells were suspended in 1 ml PBS (pH 7.4) and were subsequently analyzed using flow cytometry. For the $DiOC_6$-stained samples, PI-negative cells were excluded of the analysis. Normal and starved MSD and wild-type MEFs were analyzed at the same passage and treated in the same way. At least 10 000 cells were analyzed for each sample. The experiments were performed at least in triplicate, and all statistical analyses were performed using Stat-View 5.0 (Statsoft, USA).

Electron microscopy analysis

MEFs were fixed at room temperature, in 2.5% glutaraldehyde (Polysciences, Inc., Warrington, PA, USA), 0.1 M sodium cacodylate–HCl buffer, pH 7.3, for 10 min, scraped off the dish, pelletted by centrifugation and postfixed in 1% OsO4 (Polyscience) in the same buffer, for 20 min. After en bloc staining with 1% uranyl acetate for 1 h and ethanol dehydration, cells were embedded in LX112 (Polyscience). Tissue preparations were performed as previously described (26). Grey-silver sections were visualized using FEICM10 and Tecnai12G2 microscopes. Morphometry assessment of both number and size of the autophagosomes in MSD and wild-type MEFs was performed by the point intersection method.

Assay of proteasome activity

Chymotrypsin-like activity of 20S proteasomes was measured on brain homogenates using Suc-LLVY-AMC as substrate (20S proteasome activity assay kit; Chemicon).

Data analysis

Data were analyzed by one-way ANOVA (analysis of variance). A P-value <0.05 was considered to be statistically significant. Odds ratios for co-localization LAMP1-LC3 were determined by unconditional logistical regression analysis, using the general log-linear analysis option of *SPSS* 9 software (SPSS, Chicago).

SUPPLEMENTARY MATERIAL

Supplementary Material is available at HMG Online.

ACKNOWLEDGEMENTS

We are grateful to G. Andria, P. Ducy, G. Karsenty and R. Sitia for critical reading of the manuscript, to M. Mizuguchi for human LC3B, to P.Luzio for GFP-lgp120, and to R. Tsien for mCherry. C. Settembre is the recipient of a pre-doctoral fellowship of the European School of Molecular Medicine (SEMM).

Conflict of Interest statement. The authors declare that they have no competing financial interests.

FUNDING

Financial support from the Italian Telethon Foundation is gratefully acknowledged. We are also grateful to MRC (Grant to D.C.R. and studentship for L.J.), Wellcome Trust (Senior Fellowship in Clinical Science to D.C.R.), MIPAF (grant to A.B.), FIRB and MIUR (grants to C.T.) for funding. Electron microscopy has been performed at the Telethon facility for EM (grant GTF03001 to C.T.).

REFERENCES

1. Futerman, A.H. and van Meer, G. (2004) The cell biology of lysosomal storage disorders. *Nat. Rev. Mol. Cell. Biol.*, **5**, 554–565.
2. Jeyakumar, M., Dwek, R.A., Butters, T.D. and Platt, F.M. (2005) Storage solutions: treating lysosomal disorders of the brain. *Nat. Rev. Neurosci.*, **6**, 713–725.
3. Cardone, M., Polito, V.A., Pepe, S., Mann, L., D'Azzo, A., Auricchio, A., Ballabio, A. and Cosma, M.P. (2006) Correction of Hunter syndrome in the MPSII mouse model by AAV2/8-mediated gene delivery. *Hum. Mol. Genet.*, **15**, 1225–1236.
4. Hemsley, K.M. and Hopwood, J.J. (2005) Development of motor deficits in a murine model of mucopolysaccharidosis type IIIA (MPS-IIIA). *Behav. Brain Res.*, **158**, 191–199.
5. Fraldi, A., Hemsley, K., Crawley, A., Lombardi, A., Lau, A., Sutherland, L., Auricchio, A., Ballabio, A. and Hopwood, J. (2007) Functional correction of CNS lesions in a MPS-IIIA mouse model by intracerebral

AAV-mediated delivery of sulfamidase and SUMF1 genes. *Hum. Mol. Genet.*, 2007; doi: 10.1093/hmg/ddm223.
6. Settembre, C., Annunziata, I., Spampanato, C., Zarcone, D., Cobellis, G., Nusco, E., Zito, E., Tacchetti, C., Cosma, M.P. and Ballabio, A. (2007) Systemic inflammation and neurodegeneration in a mouse model of multiple sulfatase deficiency. *Proc. Natl Acad. Sci. USA*, **104**, 4506–4511.
7. Mizushima, N., Ohsumi, Y. and Yoshimori, T. (2002) Autophagosome formation in mammalian cells. *Cell. Struct. Funct.*, **27**, 421–429.
8. Rubinsztein, D.C. (2006) The roles of intracellular protein-degradation pathways in neurodegeneration. *Nature*, **443**, 780–786.
9. Komatsu, M., Waguri, S., Chiba, T., Murata, S., Iwata, J., Tanida, I., Ueno, T., Koike, M., Uchiyama, Y., Kominami, E. *et al.* (2006) Loss of autophagy in the central nervous system causes neurodegeneration in mice. *Nature*, **441**, 880–884.
10. Hara, T., Nakamura, K., Matsui, M., Yamamoto, A., Nakahara, Y., Suzuki-Migishima, R., Yokoyama, M., Mishima, K., Saito, I., Okano, H. *et al.* (2006) Suppression of basal autophagy in neural cells causes neurodegenerative disease in mice. *Nature*, **441**, 885–889.
11. Cosma, M.P., Pepe, S., Annunziata, I., Newbold, R.F., Grompe, M., Parenti, G. and Ballabio, A. (2003) The multiple sulfatase deficiency gene encodes an essential and limiting factor for the activity of sulfatases. *Cell*, **113**, 445–456.
12. Dierks, T., Schmidt, B., Borissenko, L.V., Peng, J., Preusser, A., Mariappan, M. and von Figura, K. (2003) Multiple sulfatase deficiency is caused by mutations in the gene encoding the human C(alpha)-formylglycine generating enzyme. *Cell*, **113**, 435–444.
13. Bhattacharyya, R., Gliddon, B., Beccari, T., Hopwood, J.J. and Stanley, P. (2001) A novel missense mutation in lysosomal sulfamidase is the basis of MPS III A in a spontaneous mouse mutant. *Glycobiology*, **11**, 99–103.
14. Kabeya, Y., Mizushima, N., Ueno, T., Yamamoto, A., Kirisako, T., Noda, T., Kominami, E., Ohsumi, Y. and Yoshimori, T. (2000) LC3, a mammalian homologue of yeast Apg8p, is localized in autophagosome membranes after processing. *EMBO J.*, **19**, 5720–5728.
15. Tanaka, Y., Guhde, G., Suter, A., Eskelinen, E.L., Hartmann, D., Lullmann-Rauch, R., Janssen, P.M., Blanz, J., von Figura, K. and Saftig, P. (2000) Accumulation of autophagic vacuoles and cardiomyopathy in LAMP-2-deficient mice. *Nature*, **406**, 902–906.
16. Boland, B. and Nixon, R.A. (2006) Neuronal macroautophagy: from development to degeneration. *Mol. Aspects Med.*, **27**, 503–519.
17. Yamamoto, A., Tagawa, Y., Yoshimori, T., Moriyama, Y., Masaki, R. and Tashiro, Y. (1998) Bafilomycin A1 prevents maturation of autophagic vacuoles by inhibiting fusion between autophagosomes and lysosomes in rat hepatoma cell line, H-4-II-E cells. *Cell. Struct. Funct.*, **23**, 33–42.
18. Ravikumar, B., Duden, R. and Rubinsztein, D.C. (2002) Aggregate-prone proteins with polyglutamine and polyalanine expansions are degraded by autophagy. *Hum. Mol. Genet.*, **11**, 1107–1117.
19. Narain, Y., Wyttenbach, A., Rankin, J., Furlong, R.A. and Rubinsztein, D.C. (1999) A molecular investigation of true dominance in Huntington's disease. *J. Med. Genet.*, **36**, 739–746.
20. Webb, J.L., Ravikumar, B., Atkins, J., Skepper, J.N. and Rubinsztein, D.C. (2003) Alpha-synuclein is degraded by both autophagy and the proteasome. *J. Biol. Chem.*, **278**, 25009–25013.
21. Nixon, R.A. (2006) Autophagy in neurodegenerative disease: friend, foe or turncoat? *Trends Neurosci.*, **29**, 528–535.
22. Komatsu, M., Ueno, T., Waguri, S., Uchiyama, Y., Kominami, E. and Tanaka, K. (2007) Constitutive autophagy: vital role in clearance of unfavorable proteins in neurons. *Cell Death Differ.*, **14**, 887–894.
23. Zatloukal, K., Stumptner, C., Fuchsbichler, A., Heid, H., Schnoelzer, M., Kenner, L., Kleinert, R., Prinz, M., Aguzzi, A. and Denk, H. (2002) p62 Is a common component of cytoplasmic inclusions in protein aggregation diseases. *Am. J. Pathol.*, **160**, 255–263.
24. Bjorkoy, G., Lamark, T., Brech, A., Outzen, H., Perander, M., Overvatn, A., Stenmark, H. and Johansen, T. (2005) p62/SQSTM1 forms protein aggregates degraded by autophagy and has a protective effect on huntingtin-induced cell death. *J. Cell Biol.*, **171**, 603–614.
25. Kim, I., Rodriguez-Enriquez, S. and Lemasters, J.J. (2007) Selective degradation of mitochondria by mitophagy. *Arch. Biochem. Biophys.*, **462**, 245–253.
26. Koike, M., Shibata, M., Waguri, S., Yoshimura, K., Tanida, I., Kominami, E., Gotow, T., Peters, C., von Figura, K., Mizushima, N. *et al.* (2005) Participation of autophagy in storage of lysosomes in neurons from mouse models of neuronal ceroid-lipofuscinoses (Batten disease). *Am. J. Pathol.*, **167**, 1713–1728.
27. Jennings, J.J., Jr, Zhu, J.H., Rbaibi, Y., Luo, X., Chu, C.T. and Kiselyov, K. (2006) Mitochondrial aberrations in mucolipidosis Type IV. *J. Biol. Chem.*, **281**, 39041–39050.
28. Neufeld, E.F. and Muenzer, J. (2001) The mucopolysaccharidoses. *The Metabolic and Molecular Basis of Inherited Disease*. Mc Graw-Hill, New York, pp. 3421–3452.
29. Cao, Y., Espinola, J.A., Fossale, E., Massey, A.C., Cuervo, A.M., MacDonald, M.E. and Cotman, S.L. (2006) Autophagy is disrupted in a knock-in mouse model of juvenile neuronal ceroid lipofuscinosis. *J. Biol. Chem.*, **281**, 20483–20493.
30. Fukuda, T., Ewan, L., Bauer, M., Mattaliano, R.J., Zaal, K., Ralston, E., Plotz, P.H. and Raben, N. (2006) Dysfunction of endocytic and autophagic pathways in a lysosomal storage disease. *Ann. Neurol.*, **59**, 700–708.
31. Ko, D.C., Milenkovic, L., Beier, S.M., Manuel, H., Buchanan, J. and Scott, M.P. (2005) Cell-autonomous death of cerebellar purkinje neurons with autophagy in Niemann-Pick type C disease. *PLoS Genet.*, **1**, 81–95.
32. Pacheco, C.D., Kunkle, R. and Lieberman, A.P. (2007) Autophagy in Niemann-Pick C disease is dependent upon Beclin-1 and responsive to lipid trafficking defects. *Hum. Mol. Genet*, **16**, 1495–1503.
33. Boya, P., Gonzalez-Polo, R.A., Casares, N., Perfettini, J.L., Dessen, P., Larochette, N., Metivier, D., Meley, D., Souquere, S., Yoshimori, T. *et al.* (2005) Inhibition of macroautophagy triggers apoptosis. *Mol. Cell. Biol.*, **25**, 1025–1040.
34. Ravikumar, B., Berger, Z., Vacher, C., O'Kane, C.J. and Rubinsztein, D.C. (2006) Rapamycin pre-treatment protects against apoptosis. *Hum. Mol. Genet.*, **15**, 1209–1216.
35. Rideout, H.J., Larsen, K.E., Sulzer, D. and Stefanis, L. (2001) Proteasomal inhibition leads to formation of ubiquitin/alpha-synuclein-immunoreactive inclusions in PC12 cells. *J. Neurochem.*, **78**, 899–908.
36. Shimura, H., Hattori, N., Kubo, S., Mizuno, Y., Asakawa, S., Minoshima, S., Shimizu, N., Iwai, K., Chiba, T., Tanaka, K. *et al.* (2000) Familial Parkinson disease gene product, parkin, is a ubiquitin-protein ligase. *Nat. Genet.*, **25**, 302–305.
37. Bence, N.F., Sampat, R.M. and Kopito, R.R. (2001) Impairment of the ubiquitin-proteasome system by protein aggregation. *Science*, **292**, 1552–1555.
38. Diaz-Hernandez, M., Hernandez, F., Martin-Aparicio, E., Gomez-Ramos, P., Moran, M.A., Castano, J.G., Ferrer, I., Avila, J. and Lucas, J.J. (2003) Neuronal induction of the immunoproteasome in Huntington's disease. *J. Neurosci.*, **23**, 11653–11661.
39. Pandey, U.B., Nie, Z., Batlevi, Y., McCray, B.A., Ritson, G.P., Nedelsky, N.B., Schwartz, S.L., DiProspero, N.A., Knight, M.A., Schuldiner, O. *et al.* (2007) HDAC6 rescues neurodegeneration and provides an essential link between autophagy and the UPS. *Nature*, **447**, 859–863.